Journal of Innovative Image Processing (ISSN: 2582-4252)
www.irojournals.com/iroiip/

Enhanced Hybrid Feature Extraction and Selection based on OCT Images for Diabetic Macular Edema Classification

Minarva Devi K.[1], Murugeswari S.[2]

[1]Department of Electronics and Communication Engineering, Sri Raaja Raajan College of Engineering and Technology, Karaikudi, India.

[2]Department of Bio Medical Engineering and Technology, Syed Ammal Engineering College, Ramanathapuram, India.

E-mail: [1]minarvadevi51@gmail.com, [2]murugeskabilan@syedengg.ac.in

Abstract

In recent decades, Diabetic Macular Edema (DME) has emerged as a significant cause of vision loss among diabetic patients due to retinal fluid leakage. To address this challenge, reliable and efficient diagnostic methods are essential. The proposed methodology aims to facilitate early detection through a multi-stage process, including feature extraction, feature selection, and classification.For feature extraction, we introduce the H2A2Net model, which incorporates a Dense Spectral-Spatial Module (DSSM) that employs 3D convolutional DenseNet-inspired layers to extract spectral-spatial features. This is complemented by a Hybrid Resolution Module (HRM) designed to achieve fine spatial detail through a multi-scale process. Additionally, a Double Attention Module (DAM) is implemented to capture global and cross-channel interactions, utilizing both pixel-wise and channel-wise attenuation. Feature selection is conducted using Cuckoo Search Spider Monkey Optimization (CSSMO), which effectively processes both local and global searches to enable efficient selection of high-value features. In the classification phase, a hybrid AdaBoost-Backpropagation Neural Network (BPNN) model is employed, where BPNNs function as weak classifiers whose outputs are iteratively boosted to create a strong ensemble. Experimental results on the CUHK dataset demonstrate that the proposed method achieves an accuracy of 97.4%, a recall of 97.6%, a

DOI: https://doi.org/10.36548/jiip.2025.2.004
Received: 12.04.2025, received in revised form: 10.05.2025, accepted: 24.05.2025, published: 03.06.2025

specificity of 97%, and an F1-score of 98%. These outcomes surpass those of existing state-of-the-art methods, indicating that the proposed approach offers enhanced robustness and efficiency for DME classification.

Keywords: DME Classification, OCT Dataset, H^2A^2 Feature Extraction, Feature Selection, Accuracy.

1. Introduction

Diabetic Macular Edema (DME) is a serious vision-related condition affecting individuals with diabetes, leading to severe visual impairment. In the retina, fluid accumulates in the macula due to leakage from damaged blood vessels and elevated blood sugar levels. Diabetic Retinopathy (DR) is associated with DME and can result in significant vision loss or even blindness if not adequately treated. Furthermore, DME poses major health concerns, adversely impacting cardiovascular, nerve, immune, and digestive health. Statistics indicate that DME affects between 4.2% and 7.9% of individuals with type 1 diabetes, while it affects 1.4% to 12.8% of those with type 2 diabetes.

DME is characterized by retinal thickening, hard exudates, microaneurysms, and hemorrhages in the macula. Two common imaging methods used for its detection are Fundus Photography and Optical Coherence Tomography (OCT). Fundus Photography provides detailed retinal images that facilitate the identification of abnormalities. In contrast, OCT delivers high-resolution cross-sectional images that allow for the visualization of retinal thickness, fluid accumulation, and other changes, aiding in the assessment of severity and informing clinical decisions.

Although OCT is effective in identifying DME, it is not optimal for the early detection of affected regions. There is a critical need for reliable and accurate early diagnosis of DME. Consequently, machine learning (ML) and deep learning (DL) have emerged as promising tools in medical imaging, offering high accuracy. Notably, Convolutional Neural Networks (CNNs) are employed to analyze spatial structures in images due to their layered architecture. Inception Networks capture multi-scale features to recognize patterns at various scales simultaneously. Additionally, attention mechanisms enhance the ability to detect indirect signs. Transfer learning, utilizing pre-trained models, enhances accuracy while requiring fewer labeled data.

Each technique possesses unique strengths, collectively enabling faster and more accurate detection of DME.

This work presents a hybrid method wherein the H2A2 method is employed for feature extraction, the CSSMO method is utilized for relevant feature selection, and the Adaboost-BPNN model is applied for classifying OCT images for DME diagnosis. The performance of the proposed method is validated against classification metrics, demonstrating superior results compared to traditional methods. The significance of this research lies in its capacity to enhance early diagnosis through advanced deep learning and feature extraction techniques. The integration of Principal Component Analysis (PCA) for dimensionality reduction, alongside the use of DenseNet with the Adaboost classifier, improves both accuracy and computational efficiency, which are essential for clinical decision support systems. This work is structured as follows: related works are discussed in Section 2, the proposed methodology in Section 3, results in Section 4, and conclusions in Section 5.

2. Related Works

Garcia-Nonoal et al. [8] introduced the ConvUNeXt model to classify hard exudates (HaEx) for DME. RetinaNet is used to localize the optic disc (OD) with an accuracy of 99.38%. Thanikachalam et al. [9] developed an Artificial Neural Network (ANN) to classify DME and extract features using an Adaptive Gabor Filter (AGF). The Random Forest (RF) is used to select features with 97.91% accuracy.

Fujiwara et al. [10] classified DME based on the location and size of fluid areas in the retina. It also explored how these fluid characteristics correlated with visual acuity (VA) using en-face OCT images created by swept-source OCT. Im, J. H., et al. [11] conducted a meta-analysis to determine the prevalence of DME using OCT. The pooled frequency was 5.47% worldwide with rates of 5.81% in low- to middle-income countries and 5.14% in high-income countries. Liu et al. [12] identified DME based on retinal thickening or fluid by using a DL system. This system was compared to expert evaluations and achieved 80% specificity and 81% sensitivity. To address DME issues, Guo et al. [13] presented an automatic detection and grading method using CNN. It improved stability and reliability in the diagnosis of DME.

Kumar et al. [14] used the DenseNet121 model for feature extraction and processed it with fully connected layers for classification. It attained an accuracy of 86.4%, demonstrating

its effectiveness in DME classification. da Costa et al. [15] developed a VGG-19 model for classification using OCT images. This model attained 82.60% accuracy and 92.03% AUROC, showcasing its robustness in DME classification. Hughes-Cano et al. [16] applied transfer learning on OCT, scalogram and fundus images to identify DME. This method performed well, attaining a 93% AUC and 89% F1-score, respectively. Wu et al. [17] developed a DL method to classify DME patterns in OCT images. It achieved an accuracy of 95.9% and attained a higher reliability. Kaymak et al. [18] used AlexNet for classification into healthy, dry AMD, wet AMD and DME. This method attained an accuracy of 99.6% and showed superior performance compared to.

3. Materials and Methods

3.1 Dataset Description

An OCT image dataset is gathered from two universities, namely the Singapore Eye Research Institute (SERI) and the Chinese University of Hong Kong (CUHK) respectively. SERI dataset has labeled 16 DME cases and 16 normal cases. The CUHK dataset includes 416 DME cases and 7,916 normal cases, numbers. To address the data imbalance, the data augmentation technique is applied to the DME cases. Every volume consists of 128 B-scan slices of 1024×512 pixels. All OCT datasets are used to train the model with grades and label them as normal or DME-affected.

4. Proposed Methodology

The proposed methodology is presented to classify a DME by performing H^2A^2Net feature extraction, CSSMO-based feature selection, and the AdaBoost-BPNN classification, respectively. This proposed approach offers a reliable DME classification with accurate diagnostics and enhances patient outcomes.

4.1 Feature Extraction

Figure 1 shows the H^2A^2Net architecture, which is used for feature extraction. The H^2A^2 model consists of PCA, DSSM, HRM, and DAM, respectively [19]. Initially, PCA is used as a pre-processing step that minimizes data dimensionality and speeds up training without any data loss. Then, the PCA provides the output as a processed 3D cube, which is is fed as

input to the DSSM module. This PCA helps to focus the spectral characteristics most relevant to DME. Its primary function is to transform the original high-dimensional dataset into a lower-dimensional subspace and preserve the most informative features. By capturing the directions of maximum variance, PCA eliminates redundancy and noise. This not only accelerates the training process but also enhances the classifier's performance by focusing on the most discriminative features.

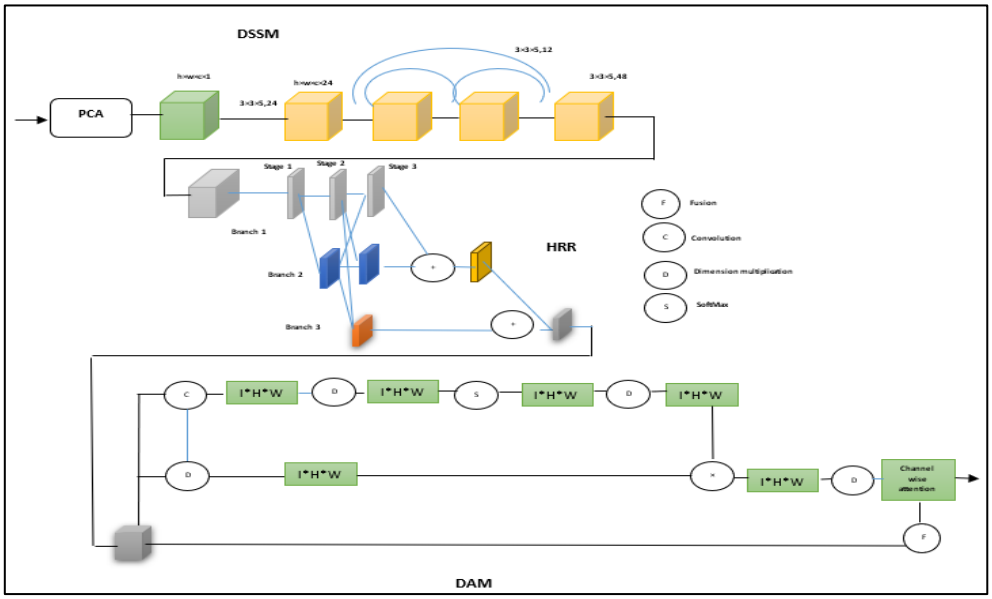

Figure 1. H^2A^2Net Feature Extraction

4.2 DSSM Module

After PCA pre-processing, the DSSM is used, inspired by DenseNet, which has dense connectivity between layers. DenseNet is utilized in this work due to its densely connected architecture, which increases feature reuse and mitigates vanishing gradients. This is especially beneficial in clinical imaging, where subtle variations are critical for diagnosis. The architecture allows for efficient learning from limited clinical datasets by improving gradient flow and reducing parameters compared to traditional CNNs. In this module, 3D convolutional layers are used to capture spectral and spatial features within the data simultaneously. Each convolution layer employs a 3D filter that allows it to extract features across both spatial dimensions (height and width) and the spectral dimension. Figure 1 shows convolution kernels with a 3×3×5 size, where the first 2-Dimensions focus on spatial filtering while the 3-D dimensions capture spectral variations. This joint spectral-spatial processing is used for DME

as the condition involves subtle changes in both spatial structure (such as the appearance of fluid pockets) and spectral characteristics. The dense connections in DSSM mean that each layer's output is concatenated with subsequent layers, allowing information to flow more freely through the network and promoting feature reuse. This DSSM helps retain lower-level spectral details and builds up multi-layered representation to capture both micro-level features (like small fluid pockets) and broader patterns in the retina.

4.3 HRM Process

The next module is HRM, which is designed to capture both fine-grained spatial details and broader semantic patterns by processing data at multiple resolutions. The HRM consists of three branches, each handling the input data at different scales: high, medium, and low resolution. It uses convolutional operations to extract features at various resolutions. The high-resolution processing detects fine details and small edema pocket changes. The medium-resolution processing captures moderate spatial patterns, while the low-resolution processing identifies high-level features across larger retinal regions. By processing data at various scales, it can address both small-scale and larger pattern detection. Then the outputs are combined using upsampling and downsampling operations to integrate both local and global data, ensuring precise spatial positioning and broader semantic data while effectively capturing diverse features related to DME.

4.4 DAM Process

The DAM is the final module in this H^2A^2 Architecture that improves it on relevant spatial and spectral features using pixel-wise attention and channel-wise attention, respectively. The pixel-wise attention is processed as a global spatial dependency based on relationships between individual pixels. By considering these relations, pixel-wise attention can detect indirectly spatially distributed features of DME. Meanwhile, channel-wise attention uses a spectral data channel to permit the channel's particular data to detect retinal abnormalities. By choosing weighting channels, channel-wise attention focuses on the most diagnostically valuable data. Therefore, this attention process prioritizes spatial and spectral features that ultimately enhanceits ability to detect and localize DME accurately.

4.5 CSSMO Feature Selection

Normally, the optimization algorithms are applied to obtain a solution for real world problems [20]. The CSSMO method is inspired by both Cuckoo Search and Spider Monkey Optimization. It is designed to explore and exploit search spaces to process a feature selection efficiently [21]. The CSSMO are validated with several steps that is given in the following.

Step 1: Initialization

1. Define the initial population P in the search space.
2. Set the control parameters:
    - LocalLeaderLimit: Limit for local leaders before redirection.
    - GlobalLeaderLimit: Limit for global leaders before population restructuring.
    - Perturbation Rate (pr): Controls the diversification in solution updates.
3. Evaluate the fitness for each individual $f(x_i)$

Step 2: Leader Selection

1. Identify the global leader G based on the highest fitness f(G) in the population.
2. Assign local leaders L in smaller groups to explore nearby solutions

Step 3: Iterative Optimization (Loop until Termination Criterion is Met)

In this phase, the process includes both the Local Leader Phase (LLP) and the Global Leader Phase (GLP).

In LLP, individuals update their positions using Equation 1.

$$x_i(t+1) = x_i(t) + r_1(L - x_i(t)) + r_2(x_j(t) - x_i(t)) \quad (1)$$

Where $x_i(t)$ denotes Self-experience, L represents the local leader's influence, r1 and r2 are random values between [0,1], xj represents randomly selected member within the same group.

- **Fitness-based Greedy Selection**

Each new position xi(t+1) is evaluated based on fitness f(xi(t+1)). If the new position has a better fitness than the previous one, it is retained.

- **Probability Calculation**

A probability probi is calculated to select individuals in GLP that is calculated based on fitness as shown in (Eq.2):

$$Prob_i = \frac{f(x_i(t+1)}{\sum_{j=1}^{N}(x_j(t+1)} \quad (2)$$

In GLP, individuals update positions based on Equation 3.

$$x_i(t+1) = x_i(t) + r_3(G - x_i(t)) + r_4(x_k(t) - x_i(t)) \quad (3)$$

Where G denotes global leader experience, r3 and r4 are random values in [0,1],xk denotes an another random member of the population.

After each GLP iteration, local and global leaders are updated based on greedy selection.

- **Adaptive Foraging and Group Splitting**

1. Local Leader Constraint (LocalLeaderLimit): When a local leader's performance reaches its limit, all members in that group adopt the cuckoo search local search method to diversify search directions.

2. Global Leader Constraint (GlobalLeaderLimit): If the global leader reaches its limit, the population divides into smaller groups. Each group continues independently in LLP and GLP to maintain a balance of exploration and exploitation.

Step 4: Termination and Final Solution

The algorithm repeats the LLP and GLP cycles until the termination criterion (e.g., maximum number of iterations, target fitness level) is satisfied. The solution with the best fitness f(G) at termination is output as the optimal feature selection for the given dataset.

4.6 AdaBoost-BPNN based Classification

The AdaBoost-BPNN classifier is designed to improve the accuracy and robustness of classification in DME OCT images. In this proposed work, AdaBoost is used as the primary ensemble technique, while BPNN acts as individual weak classifiers within the ensemble [22]. Each BPNN is processed as a separate model and generates predictions based on selected features from the dataset. This approach achieves a powerful ensemble model where weak classifiers are improved to build a strong classifier iteratively, resulting in robust and accurate DME classification.

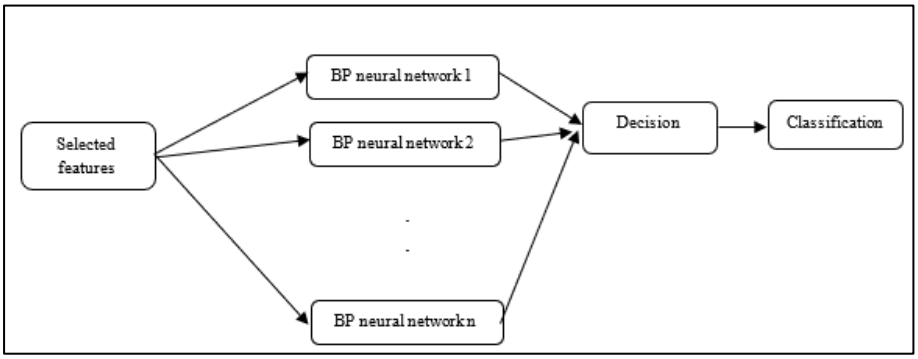

Figure 2. AdaBoost-BPNN Classifier

The figure shows an Adaboost-BPNN classification that starts with selected features as input. These features are processed in parallel by multiple BPNN (labeled as BP neural network 1, 2, ..., n). Each network is used to classify the features independently and produces an output. The outputs from all BPNNs are then aggregated in a decision strategy module. This module consolidates the results from every network to make a final classification decision. The final output is classified as severity of DME or normal. Therefore, this proposed method processes more informative features and corrects errors iteratively through its boosting process, achieving higher accuracy in DME detection.

AdaBoost was integrated as a classifier following DenseNet-based feature extraction to increase classification accuracy. AdaBoost's ability to focus on misclassified samples helps address class imbalance and improve robustness. This hybrid approach uses DenseNet for deep feature representation and AdaBoost for refined classification decision-making.

5. Result And Discussion

The proposed model for DME classification was evaluated using a 70-30 split of the datase,t with 70% of the data allocated for training and 30% for testing. This split ensures that the model has sufficient data to learn patterns while maintaining a separate test set for unbiased performance evaluation. The outlier data points are identified using statistical methods such as the interquartile range (IQR) and z-score analysis and are adjusted based on clinical relevance. Classification error refers to the proportion of incorrectly predicted instances compared to the total instances and is calculated as:

$$classification\ error = \frac{Number\ of\ Incorrect\ Predictions}{Total\ number\ of\ Predictions} \times 100\% \quad (4)$$

In this work, the error was calculated by comparing the predicted class labels with the actual labels on the test dataset. The fitness curve of CSSMO-based feature selection is shown in Figure 3. The y-axis represents the classification error (fitness value), and the x-axis denotes the number of iterations.

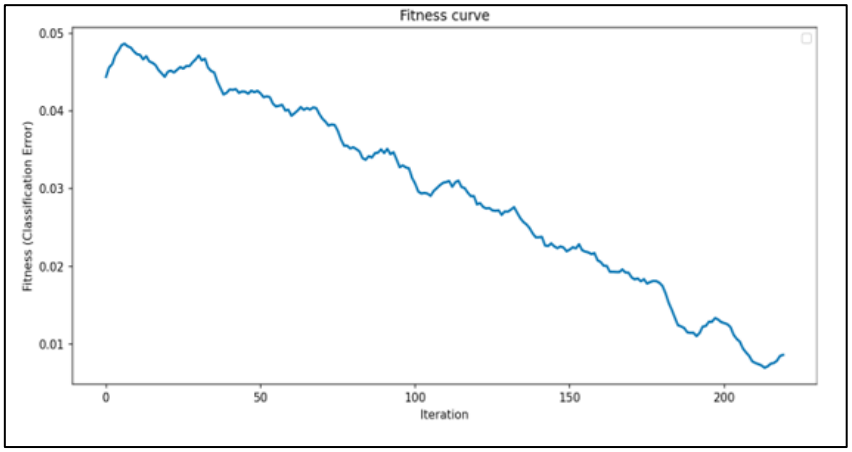

Figure 3. Fitness Curve of CSSMO

The fitness curve shows a clear downward trend in classification error over the course of 225 iterations. This convergence behavior confirms that CSSMO exhibits a strong global search capability and stability in minimizing the objective function. The low final fitness value proves that the selected features significantly increase classification performance. The model loss and accuracy validation are given in Figure 4. The minimal gap between training and validation metrics indicates that the model is not only accurate but also generalizes well to new data.

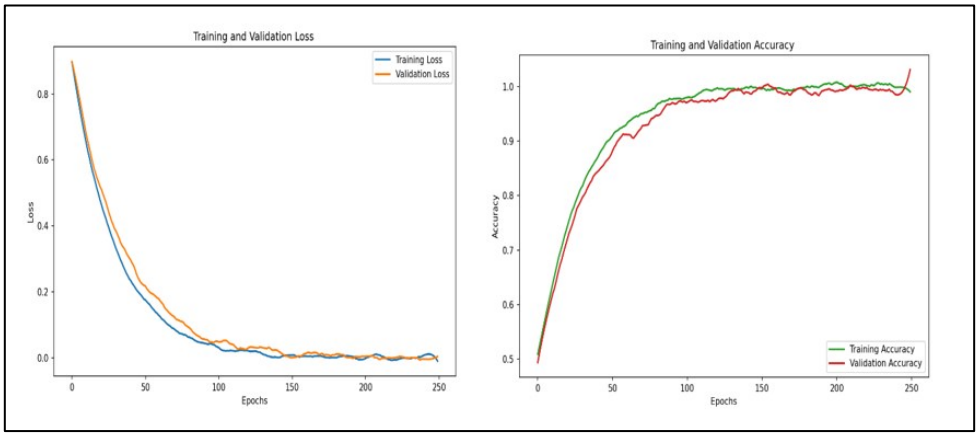

Figure 4. Model Validation and Loss Curve

To evaluate the model's effectiveness, the classification metrics are analysed namely Precision, Recall, Specificity, Accuracy and F1 Score. Each of these metrics offers unique insights into the model's strengths and potential areas for enhancement in DME classification.

Table 1. Performance Table of Classification Metrics

Metrics	Proposed	Transfer Learning	GAN	CNN-GRU	BiLSTM	BPNN	CNN
Precision (%)	98.2	95	94.5	93	92.4	90	89.8
Recall (%)	97.6	94	96	95.2	90.2	88.2	87.4
Specificity (%)	97	93.2	94.2	93.5	90.3	89.6	88.2
Accuracy (%)	97.4	95.2	94.9	93.6	92.4	88	89
F1 score (%)	98	94.6	95.2	94.7	91.3	89.6	88.6

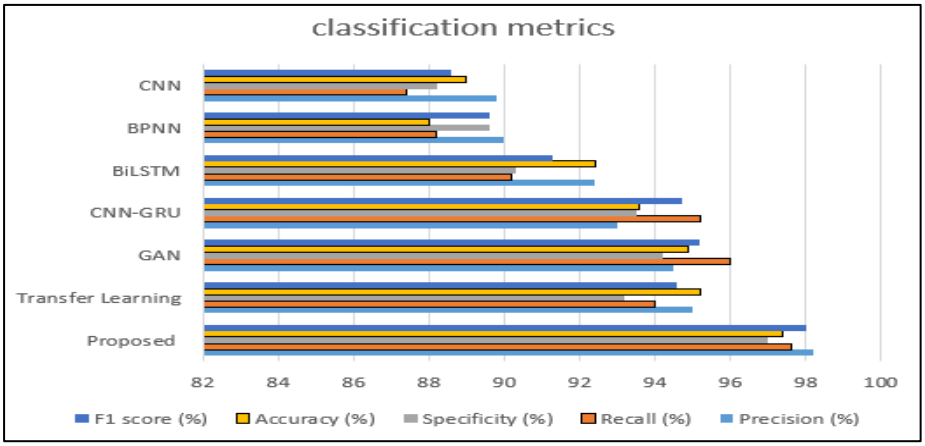

Figure 3. Overall Classification Performances

Table 1 and Figure 3 present the performance of several DL methods for DME classification. The proposed model outperforms all other metrics such as precision, recall, specificity, accuracy, and F1 score. It achieves the highest precision (98.2%) which is accurate in identifying true positive DME cases while minimizing false positives. The proposed recall (97.6%) shows its effectiveness by reducing the number of missed positive instances. It also achieves the best specificity (97%) that helps avoid false positive diagnoses. With an accuracy of 97.4%, the proposed model is highly reliable for clinical use. The F1 score stands at 98%, demonstrating its ability to handle data with precision and sensitivity. Other models like Transfer Learning, GAN and CNN-GRU also perform well in precision and recall that is next to the proposed model. Models like BiLSTM, BPNN and CNN indicate very lower accuracy in detecting DME than the proposed model.

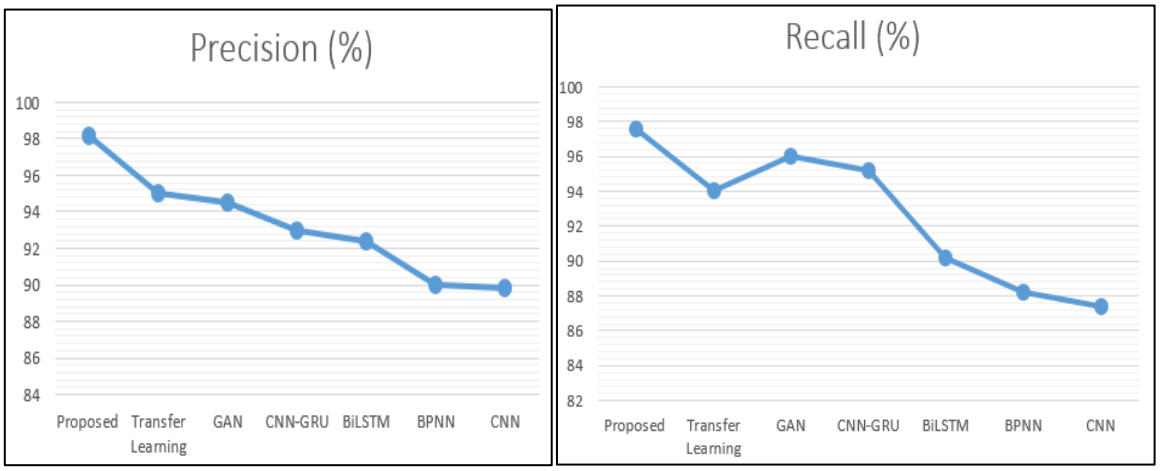

(a) (b)

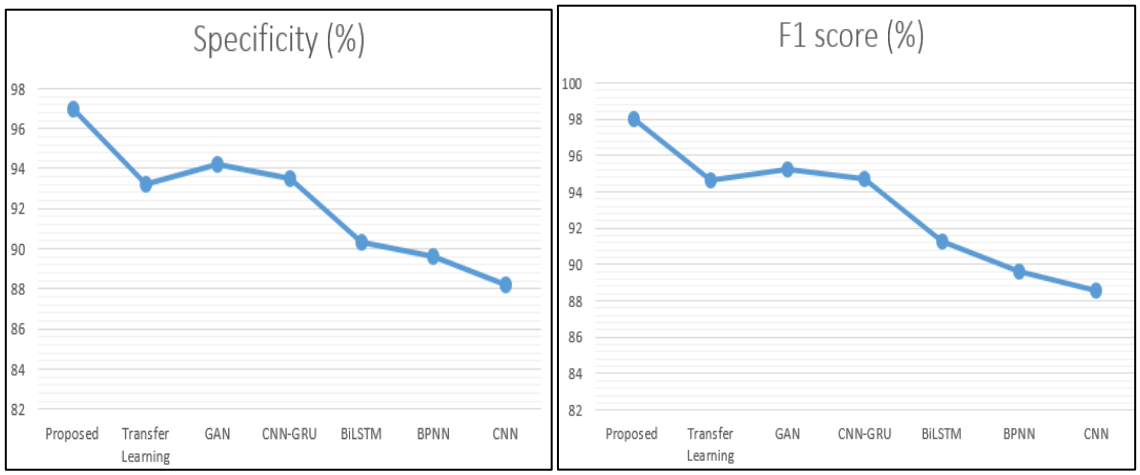

(c) (d)

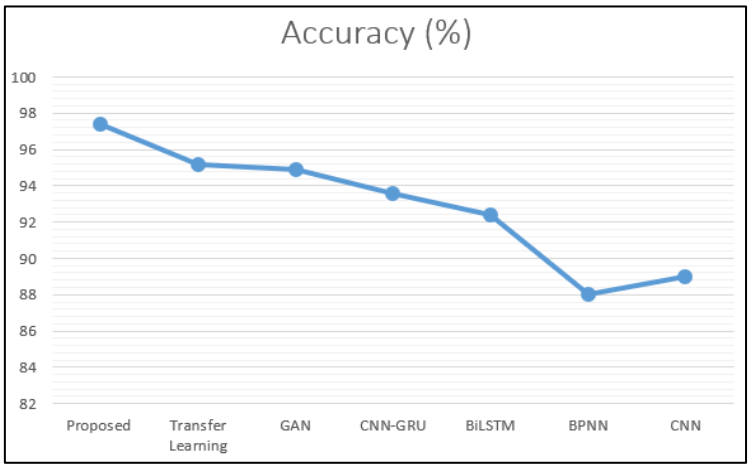

(e)

Figure 4. Graphical Representation of Classification Metrics (a) Precision, (b) Recall, (c) Specificity, (d) F1 Score and (e) Accuracy

Figure 4(a) shows the Precision metrics performances, indicating how many of the DME-positive predictions are correct. The Proposed Model has the highest precision at 98.2%, while other models like Transfer Learning (95%) and GAN (94.5%) perform well but are slightly lower. The lowest precision is observed in BPNN (90%) and CNN (89.8%), which incorrectly label non-DME cases as DME more often.

Figure 4(b) represents the Recall metrics graph, which addresses missed diagnoses. The Proposed Model has the highest recall at 97.6%, detecting nearly all DME cases. GAN and CNN-GRU also show good recall but lower scores in other metrics. In contrast, BPNN (88.2%) and CNN (87.4%) are less effective at identifying all DME cases.

Figure 4(c) shows the graphical representation of Specificity performances, illustrating how well the model avoids false positives. The Proposed Model achieves 97% specificity, and other models like GAN (94.2%) and CNN-GRU (93.5%) are also strong in specificity. Additionally, the lower specificity in BPNN (89.6%) and CNN (88.2%) suggests these models may frequently misclassify non-DME cases as DME.

Figure 4(d) presents the graphical representation of F1 Score performances, which are useful when there is data imbalance. The Proposed Model has the highest F1 score at 98%, while GAN (95.2%) and CNN-GRU (94.7%) perform well, though not as comprehensively

balanced. The lower F1 scores in BPNN (89.6%) and CNN (88.6%) indicate that these models are less reliable in balancing true positives and avoiding false positives.

Figure 4(e) shows the graphical representation of Accuracy performances, indicating the overall correctness of the model's predictions across both positive and negative cases. The Proposed Model leads with 97.4% accuracy, making it the most balanced and reliable. Transfer Learning (95.2%) and GAN (94.9%) also show good accuracy, but the lower scores of BPNN (88%) and CNN (89%) suggest these models are less dependable for accurate DME diagnosis.

Figure 5 shows the confusion matrices for the proposed model with and without the CSSMO technique. The left matrix corresponds to the model integrated with CSSMO, while the right matrix shows performance without optimization. With CSSMO, the model correctly classified 2,317 Normal and 2,035 DME samples, misclassifying only 57 Normal and 65 DME samples. This denotes a strong balance between sensitivity and specificity. In contrast, the model without CSSMO correctly predicted 2,292 Normal and 2,011 DME cases, with higher misclassification counts of 82 and 89, respectively.

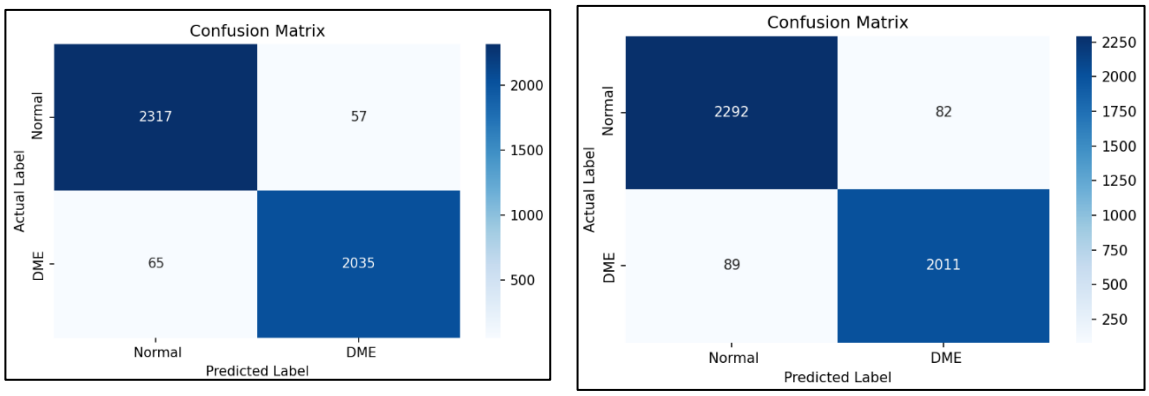

Figure 5. a) With CSSMO b) Without CSSMO

The computational analysis of the proposed model is given in Table 2. The integration of CSSMO slightly increases training time, but the inference speed remains within acceptable clinical limits and proves suitable for real-time implementation.

Table 2. Computational Analysis of the Proposed Model

Model	**Training Time (hrs)**	**Inference Time (ms/image)**	**GPU Used**
Proposed model without CSSMO	1.9	**9**	NVIDIA RTX 3090
Proposed model with CSSMO	2.3	13	NVIDIA RTX 3090

6. Conclusion

The proposed methodology demonstrates high accuracy and robustness in detecting diabetic macular edema (DME), utilizing the H2A2Net architecture for feature extraction, the CSSMO algorithm for precise feature selection, and the AdaBoost-BPNN ensemble for classification. When tested on the SERI and CUHK OCT datasets, the model exhibited significant improvements in identifying DME compared to traditional methods. The proposed model achieved a precision of 98.2%, a recall of 97.6%, a specificity of 97%, an accuracy of 97.4%, and an F1 score of 98% on these datasets. These results highlight a substantial advancement over conventional approaches, underscoring the model's effectiveness in accurately identifying DME cases while minimizing false positives. Future work will focus on expanding the model to incorporate additional imaging modalities such as fundus photography and fluorescein angiography to enhance diagnostic capabilities. Additionally, efforts will be made to optimize the model for real-time clinical deployment.

References

[1] Hui, Vivian WK, Simon KH Szeto, Fangyao Tang, Dawei Yang, Haoyu Chen, Timothy YY Lai, Ao Rong et al. "Optical coherence tomography classification systems for diabetic macular edema and their associations with visual outcome and treatment responses–an updated review." Asia-Pacific Journal of Ophthalmology 11, no. 3 (2022): 247-257.

[2] Parodi Battaglia, Maurizio, Pierluigi Iacono, Marialucia Cascavilla, Ilaria Zucchiatti, and Francesco Bandello. "A pathogenetic classification of diabetic macular edema." Ophthalmic Research 60, no. 1 (2018): 23-28.

[3] Arf, Serra, Isil Sayman Muslubas, Mumin Hocaoglu, Mehmet Giray Ersoz, Hakan Ozdemir, and Murat Karacorlu. "Spectral domain optical coherence tomography classification of diabetic macular edema: a new proposal to clinical practice." Graefe's archive for clinical and experimental ophthalmology 258 (2020): 1165-1172.

[4] Ruia, S., Saxena, S., Cheung, C. M. G., Gilhotra, J. S., & Lai, T. Y. (2016). Spectral domain optical coherence tomography features and classification systems for diabetic macular edema: a review. The Asia-Pacific Journal of Ophthalmology, 5(5), 360-367.

[5] Kulyabin, Mikhail, Aleksei Zhdanov, Anastasia Nikiforova, Andrey Stepichev, Anna Kuznetsova, Mikhail Ronkin, Vasilii Borisov et al. "Octdl: Optical coherence tomography dataset for image-based deep learning methods." Scientific data 11, no. 1 (2024): 365.

[6] Akilandeswari, A., T. Jerry Alexander, P. Ganesan, V. Janakiraman, D. Akila, and G. Sajiv. "Superpixels-based Segmentation and Classification using Modified Fuzzy C-Means Clustering and Color Features." In 2024 10th International Conference on Communication and Signal Processing (ICCSP), IEEE, 2024, 1223-1228.

[7] Jampol, Lee M. "Classifications of diabetic macular edema." European Journal of Ophthalmology 30, no. 1 (2020): 6-7.

[8] Garcia-Nonoal, Zaira, Atoany Fierro-Radilla, and Mariko Nakano. "A Comprehensive Approach for an Interpretable Diabetic Macular Edema Grading System Based on ConvUNext." Applied Sciences 14, no. 16 (2024): 7262.

[9] Thanikachalam, V., K. Kabilan, and Sudheer Kumar Erramchetty. "Optimized deep CNN for detection and classification of diabetic retinopathy and diabetic macular edema." BMC Medical Imaging 24, no. 1 (2024): 227.

[10] Fujiwara, Atsushi, Yuki Kanzaki, Shuhei Kimura, Mio Hosokawa, Yusuke Shiode, Shinichiro Doi, Kosuke Takahashi, Ryo Matoba, and Yuki Morizane. "En face image-based classification of diabetic macular edema using swept source optical coherence tomography." Scientific reports 11, no. 1 (2021): 7665.

[11] Im, James HB, Ya-Ping Jin, Ronald Chow, and Peng Yan. "Prevalence of diabetic macular edema based on optical coherence tomography in people with diabetes: A systematic review and meta-analysis." Survey of Ophthalmology 67, no. 4 (2022): 1244-1251.

[12] Liu, Xinle, Tayyeba K. Ali, Preeti Singh, Ami Shah, Scott Mayer McKinney, Paisan Ruamviboonsuk, Angus W. Turner et al. "Deep learning to detect OCT-derived diabetic macular edema from color retinal photographs: a multicenter validation study." Ophthalmology Retina 6, no. 5 (2022): 398-410.

[13] Guo, Xiaoxin, Xinfeng Lu, Baoliang Zhang, Xiaoying Hu, and Songtian Che. "Automatic detection and grading of diabetic macular edema based on a deep neural network." Retina 42, no. 6 (2022): 1095-1102.

[14] Kumar, Amit, Anand Shanker Tewari, and Jyoti Prakash Singh. "Classification of diabetic macular edema severity using deep learning technique." Research on Biomedical Engineering 38, no. 3 (2022): 977-987.

[15] da Costa, Inês Coelho, Sónia Torres-Costa, Guilherme Barbosa, Eduardo Carvalho, Marco Parente, Ana Guerra, Nilza Ramião, and Manuel Falcão. "Deep Learning Network to Distinguish Between Retinal Vein Occlusion and Diabetic Macular Edema." Investigative Ophthalmology & Visual Science 65, no. 7 (2024): 1611-1611.

[16] Hughes-Cano, J. A., Hugo Quiroz-Mercado, L. F. Hernández-Zimbrón, R. García-Franco, JF Rubio Mijangos, E. López-Star, M. García-Roa, V. C. Lansingh, U. Olivares-Pinto, and S. C. Thébault. "Improved predictive diagnosis of diabetic macular edema based on hybrid models: An observational study." Computers in Biology and Medicine 170 (2024): 107979.

[17] Wu, Tianzhu, Liting Liu, Tianer Zhang, and Xuesen Wu. "Deep learning-based risk classification and auxiliary diagnosis of macular edema." Intelligence-Based Medicine 6 (2022): 100053.

[18] Kaymak, Sertan, and Ali Serener. "Automated age-related macular degeneration and diabetic macular edema detection on oct images using deep learning." In 2018 IEEE 14th international conference on intelligent computer communication and processing (ICCP), IEEE, 2018, 265-269.

[19] Shi, Hao, Guo Cao, Youqiang Zhang, Zixian Ge, Yanbo Liu, and Peng Fu. "H2A2Net: A hybrid convolution and hybrid resolution network with double attention for hyperspectral image classification." Remote Sensing 14, no. 17 (2022): 4235.

[20] Ganesamoorthy, B. Narmadha, D. S. Sakthivel, and K. Balasubadra. "Hen maternal care inspired optimization framework for attack detection in wireless smart grid network." Int J Inf Commun Technol (IJ-ICT) 13 (2024): 123-130.

[21] Joshi, Amol Avinash, and Rabia Musheer Aziz. "A two-phase cuckoo search based approach for gene selection and deep learning classification of cancer disease using gene expression data with a novel fitness function." Multimedia Tools and Applications 83, no. 28 (2024): 71721-71752.

[22] Cai, Bingzi, Mutian Li, Huawei Yang, Chunsheng Wang, and Yougen Chen. "State of Charge Estimation of Lithium-Ion Battery Based on Back Propagation Neural Network and AdaBoost Algorithm." Energies 16, no. 23 (2023): 7824.